Proceedings of the ASME 2017 20th International Manufacturing Science and Engineering Conference
MSEC2017
June 4-8, 2017, Los Angeles, CA, USA

MSEC2017-2694

STUDYING THE MECHANISMS OF HIGH RATES OF TOOL WEAR IN THE MACHINING OF ARAMID HONEYCOMB COMPOSITES

David D. Gill[1], Derek M. Yip-Hoi, Max Meaker, Taryn Boni,
Erica L. Eggeman, Alex M. Brennen, Aidan Anderson
Western Washington University
Manufacturing Engineering Program, Engineering & Design Department
Bellingham, WA, USA
[1] Contact Author

KEYWORDS
Aramid Honeycomb Machining, Nomex Composite, Tool Wear in Milling, High Speed Video

ABSTRACT
Aramid honeycomb composite structures have revolutionized the aerospace industry by providing high strength, light weight, energy absorbing structures for many applications. To finder wider utilization, the costs of producing honeycomb structures must be reduced and one important area of focus is to reduce tool wear and increase tool life. This study began with the hypothesis that the high rate of tool wear was due to excessive tool rubbing because of the lower stiffness of this material when compared to solid materials. Tool wear measurements were taken over the life of a tool and high speed video was utilized to study the machining process. The results of the tool wear test showed a standard tool wear timeline. The video analyses showed the tool experiencing rubbing far beyond expectations due to the collapse of honeycomb cells induced by twisting far in advance of the arrival of the tool.

INTRODUCTION
Aramid honeycomb composite structures provide designers with high strength, light weight parts that are critical for increasing the fuel efficiency of transportation. Honeycomb also offers other important characteristics such as energy absorption for both sound and impact, self-extinguishing fire resistance, dielectric strength, and thermal and electrical insulation. This material is used extensively in aerospace applications and is also being used in electric vehicles, high-performance boats, and surfboards. In most current uses, the designer is limited to pieces with uniform thickness because the use of sculpted surfaces significantly increases production costs. Sculpted surfaces are currently utilized primarily in applications where aerodynamics or fluid flow require a complex or smooth surface to be presented to the flow stream. These applications include access panel covers, engine cowlings, radomes, helicopter blades, and fairings that operate during flight like landing gear doors. However, as aramid honeycomb composites are utilized for more common applications, especially those that are sold to a more mainstream consumer customer base like for electric vehicles, designers will demand that more complex surfaces be available economically, whether for function or form.

For manufacturers coming from a metals background, it could be expected that cutting honeycomb would cause virtually no tool wear. The materials are paper thin and the majority of the honeycomb structure is air having less than 4% of the volume occupied by material. However, the observed tool wear rates are quite high. With tools costing between $170-$500 each, this high rate of tool wear represents a significant cost. Therefore, investigating the causes of tool wear is the initial step toward the goal of reducing the cost of aramid honeycomb machining through the reduction of tool wear.

BACKGROUND
Composite materials have presented the aerospace industry with an opportunity to create lower mass components while also improving stiffness and strength. One method of creating high strength, low mass structures is the use of aramid honeycomb cores in a composite sandwich. Aramid honeycomb consists of high performance fibers like Kevlar, Nomex, or similar materials pressed into paper-like sheets which are then joined to form a honeycomb structure that is dipped in a phenolic resin and cured to form a matrix around the fibers. Complex, aerodynamically efficient structures require surface machining of the honeycomb core before the skin plies are added and a sandwich structure is created. Many of the structures being required in current and

next-generation airframes have tightly-toleranced shapes with complex surface geometry that require 5-axis machining of sculptured surfaces. The machining of fiber reinforced composites, found in the honeycomb core, presents special challenges to machining because of delamination of fibers from the matrix, incomplete separation of machined material (flagging) leading to re-machined material, deflection of the honeycomb wall structure, and brittle mode machining of the matrix and the embedded fibers. These factors combine to create a very abrasive machining environment that results in high rates of tool wear, a challenge that is exacerbated by the very long machining times required to shape these structures while achieving the required feature tolerances. The rate of tool wear leads to great expense because of the high cost of tools with advanced coatings and the need for rework or scrapping of parts not meeting tolerance due to worn tools.

The need to address tool wear in composite machining has been well recognized and studied in bulk and laminated (multilayer, multi-material) composite systems. Palinikumar [1] studied the rate of tool wear in glass fiber reinforced polymer, finding the cutting speed and feed rate to greatly affect the tool wear. Fiber orientation has been shown to greatly affect tool wear by Takeyama [2] especially as the fiber direction approaches the tool path direction causing the fiber to fail in shear and to place compressive stress on the flank face of the tool which produces significant heat from friction and causes excessive wear. This finding indicates one difficulty of predicting tool wear in honeycomb machining that cannot be drawn from bulk machining literature. Because of the random fiber orientation in the aramid paper used to create the honeycomb, force conditions on the tool and potentially also the rate of tool wear will vary significantly throughout the cutting process. Seeman [3] details the Nomex honeycomb production process and states that for material analysis purposes, researchers have found some level of alignment of the longer fibers of the matrix that can be seen in a bulk elastic modulus of the paper. However, from a machining standpoint, the alignment of the fibers is not regular enough to act like the ordered fibers of the bulk materials. A side view of the honeycomb paper used in this study is shown in Figure 1 where the non-uniform fiber direction is apparent. The darker vertical lines in this image are glue lines and honeycomb cell wall edges and do not indicate fiber orientation. Lopez de Lacalle [4] studied tool wear in carbon fiber reinforced polymer (CFRP) and developed methods for evaluating the tool wear on multi-toothed cutters. Much other work has also investigated glass reinforced polymers as well, but Nomex is known to be a less brittle material than these other materials, likely leading to alternative conclusions.

While the machining of aramid honeycomb is currently utilized in industry and conversations have anecdotally stated that high rates of tool wear are universally experienced, no information was found regarding any effects of the honeycomb structure, the unique properties of the aramid paper, or the effects of the highly interrupted cut and the “flagging” and re-machining of partially connected material.

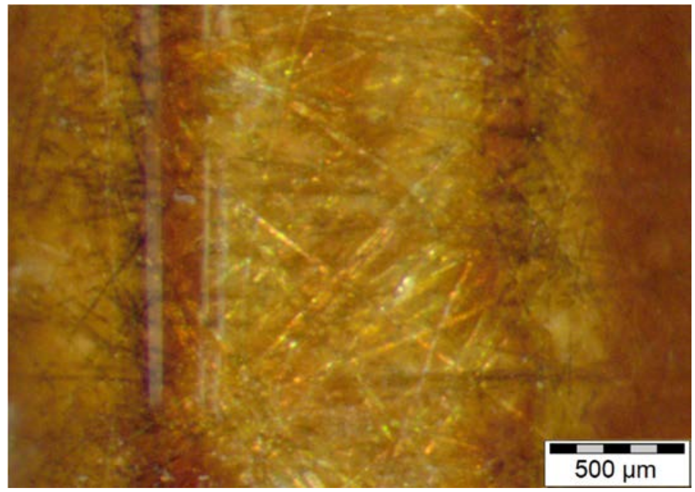

FIGURE 1. NOMEX HONEYCOMB PAPER EXHIBITS A RANDOM FIBER ORIENTATION IN THIS MICROSCOPE IMAGE

Because of the differences between honeycomb and bulk composites, especially with regard to stiffness, it is important to understand the properties and responses of honeycomb structures. Much of the strength information available on honeycomb is primarily concerned with the strength and stiffness of honeycomb composites that already have skins applied and are most concerned with the so-called “out of plane” properties, i.e. those that are along the axis of the honeycomb cells. Even when the in-plane, or shear, properties of the materials are studied, they are given for the honeycomb block as a whole. For most designers, the bulk material properties of the honeycomb are of primary concern as is evidenced by the test methods detailed in the SAE standard [5]. The material data sheet from Hexcel for HRH-10 [6] (the material used in the testing reported herein), following the SAE standard, gives mechanical properties for bulk material both in-plane and out-of-plane. But when considering the machining of honeycomb, the tool is interacting with either individual honeycomb cells or a small group of cells that are in a free condition on one end and a varying constraint condition on the lower end based on the distance from and method of mounting. These so-called meso-scale properties are of interest to researchers developing finite element models to address localized deformation in honeycomb for connectors placed in the panel [3]. Additionally, an excellent compilation of honeycomb information including the in-plane properties can be found in Gibson [7]. Not only does this reference have analysis of the materials in their undeformed state, it also contains information regarding changes that occur in the materials as the cell walls begin to collapse and bend under load. As we shall see, the bending mode of the walls is of great importance to this work.

So, while tool wear in composite machining has been studied for bulk, layered, matrix/fiber systems typically with fixed fiber orientation, it is either not well understood or not well documented for honeycomb structures which contain varying (random) fiber orientations, semi-rigid structures for machining, and interrupted (non-continuous) cutting conditions for the tool. The goal of this research was to begin to address these challenges by studying the cutting process to find the causes of tool wear in honeycomb machining.

METHOD

The hypothesis under examination with this work is that the high rate of tool wear in aramid honeycomb machining is due to the relatively low stiffness of the material causing excessive rubbing and heat generation on the tool. The planned method for testing the hypothesis was to machine aramid honeycomb materials using a baseline set of machining parameters and to remove the tool at prescribed intervals to take microscope images for the purpose of measuring tool wear.

The baseline parameters for testing, as listed in Table 1, were determined using manufacturer's recommendations [8], industry practice, and anecdotal evidence from literature. The tool used was a 12.5mm diameter Profile Cut shredder from Controx USA (Figure 2) with tool specifications listed in Table 2. The shredder is commonly used in honeycomb machining when there is a large amount of material to remove, such as in roughing steps, and for pockets and other tightly radiused features. Typically, one would use a 16-50mm diameter tool for extensive roughing of the part, but several considerations prevented the use of a larger tool. First, the spindle and collet holder being utilized would accept a maximum 12.5mm diameter tool shank and the team was concerned that a small tool shank on a larger diameter tool could cause the test results to be overwhelmed by vibration. Secondly, a smaller tool, having less surface area, will wear more quickly which reduces the length of each test and the rate of material usage. One parameter that is unique to honeycomb machining is whether the machine feed is along, against, or at an angle to the ribbon. Honeycomb is most often produced by gluing layers of material (Nomex paper, in this case) together with glue lines that shift from layer to layer. When the layers are pulled apart, the honeycomb shape is formed. The direction along the sheets of paper is defined as the ribbon direction. The Table also shows 13 passes per layer which does not complete the layer. This was done to avoid edge effects for the last cut on a layer which threatened to tear out significant portions of the layers below, potentially breaking off the most vulnerable cutting edges at the end of the tool.

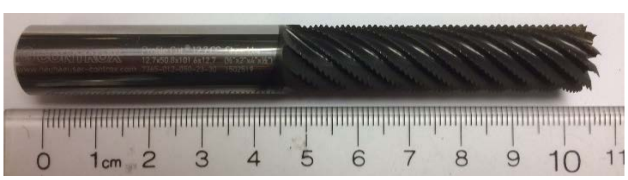

FIGURE 2. THE CONTROX PROFILE CUTTER

In order to achieve the 17,500 rpm spindle speed recommended by the tool manufacturer, a mounting plate was designed and fabricated to attach a 0.5 KW router to the Z axis of a Haas VF-2 vertical milling machine. The mounting plate was designed to be quite rigid during operation, but was also designed to allow the lead angle (the tilt along the direction of tool travel) of the tool to be changed from -25° to 25° in 5° increments. Figure 3 shows the router mounted on the mounting plate and attached to the Haas mill's Z axis. The router chosen has ample horsepower and was selected because of having high quality bearings that give good spindle rotational characteristics and good rigidity exhibiting minimal axial movement. The ability to impart lead angle to the tool was important for emulating the practices used in 5-axis machining of honeycomb material on the 3-axis machine used for testing. The machining was limited to a single direction but this would have been true in any case because of the desire to take video of the process and the possible locations for mounting a camera. The router's spindle speed was measured using a Fluke 810 Vibration Tester and adjusted to 17,500rpm. The axes of the Haas VF-2 milling machine were used for the motion control and positioning of the tool as it traversed the honeycomb material.

FIGURE 3. ROUTER MOUNTED ON Z AXIS OF THE HAAS VERTICAL MILL - SHOWN WITH 5° LEAD ANGLE

TABLE 1. BASELINE MACHINING PARAMETERS FOR TOOL WEAR TEST

Machining Parameter	Baseline Value
Spindle Speed	17,500rpm
Axis Feedrate	3,810mm/min (150ipm)
Cutting Strategy	Conventional (up cutting)
Ribbon Orientation	With (along) the ribbon
Axial Depth of Cut	9.53mm (0.375")
Radial Stepover	75% tool dia. = 19.05mm
Cut length (sample length)	540mm
Passes per layer (approx.)	13
Layers per test piece	4

TABLE 2. TOOL PARAMETERS FOR TOOL WEAR TESTS

Tool Parameter	Value
Type	Controx Profile Cut 17035
Diameter	12.5mm (0.5")
Cut Length	50.8mm
Overall Length	101.6mm
Helical Cutting Flutes	10
Coating	AWAC3

RESULTS AND ANALYSIS

The initial testing was conducted over a 2 day period with the total time in cut being 95.7 minutes. During the test, standard videos and still images were taken and these images appeared to confirm the hypothesis that the lack of localized stiffness of the honeycomb caused extended contact with the tool. However, because the video in the initial testing was taken at standard frame rates of 30 frames per second, two adjacent frames of the video included tool movement of 2.12mm from frame to frame and the tool had completed 9.7 revolutions.

During the course of the cutting test, the tool was removed from the spindle for inspection with a microscope at routine intervals. The four representative tool images of Figure 4 show the same tool flute taken at 4 significant times during the cutting test. The images were taken of the same tooth and with the tool rotated to the same position. An algorithm was written that converted the images to black or white, performed some rotational and positional correction based on features away from the cutting surface, and then calculated the area of black pixels (representing the tool) in the image.

Figure 5 shows the difference in the number of pixels in the images from the initial tool image. The method was first tested for repeatability by installing the same tool repeatedly to determine whether the tool's angle and position could be achieved image to image and the agreement was found to be good. However, in the machining process, fiducials near the teeth wore away and changed making a microscopic view have little value quantitatively, though qualitatively the wear process could be observed. This made a macroscopic view of a larger portion of the tool necessary for quantifying the wear. In the macroscopic view, the change due to wear was a small percentage of the total image which increased the uncertainty of the measurements.

The overall progression of tool wear is significant and.is shown in the tool images of Figure 4 with the graph in Figure 5. The graph is a measurement of the same set of teeth on a single flute measured at time intervals throughout the cutting process. These images show that the lowest teeth on the tool exhibited significant wear and rounding during the first 7.4 minutes of cut time which is equivalent to 28.1m of linear feed. Some of this rounding is indicated by the arrow in the 7.4min image. The wear then leveled out until 73.6 minutes (280.4 meters of linear feed) at which time a significant loss of tool material occurred very quickly through the shedding of cutting teeth (not shown in Figure 4 but seen on other cutting flutes.) At 95.7 minutes (364.6m linear feed) the tool began to wrap chips on a routine basis rather than cutting them loose. This chip wrap caused the tool to rip sections of honeycomb out of the part leaving a gaping hole in the honeycomb cells below the machined surface. The test was stopped at this point. The apparent drop-off in the wear on the graph at the very end was due to failure of the algorithm to adequately cope with significant tool edge loss in the image alignment process.

The team also took microscope image of the same teeth throughout the process and attempted to measure edge radii throughout the process, but the repeatability of these measurements did not achieve statistical significance. This was primarily due to the tools not wearing in perfect circular arcs but rather in elliptical or parabolic or irregular arcs requiring too much subjectivity in selecting foci and radii to achieve repeatable results.

The pixel image tests showed that there is a significant amount of wear occurring during the machining process in a relatively short period of time. It is important to consider that in most machining, the cutting speed (and thus the spindle speed) is the largest factor in heat generation and wear failure. These tests were done at 17,500rpm which is near the upper limit of the tool manufacturer's suggested spindle speed range. The tests were done at these speeds because it is the lower end of the speed capability of most commercial spindles on 5-axis routers designed for cutting composite materials.

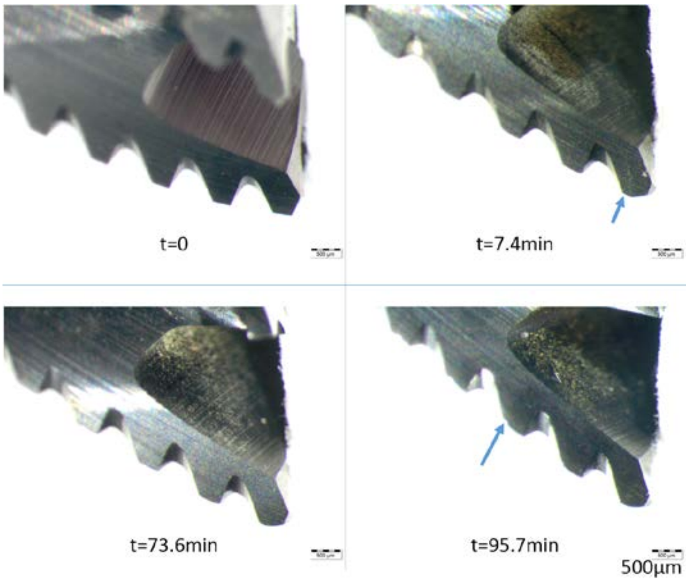

FIGURE 4. MICROSCOPE VIEW OF TOOL TAKEN AT FOUR IMPORTANT TIMES DURING CUTTING PROCESS

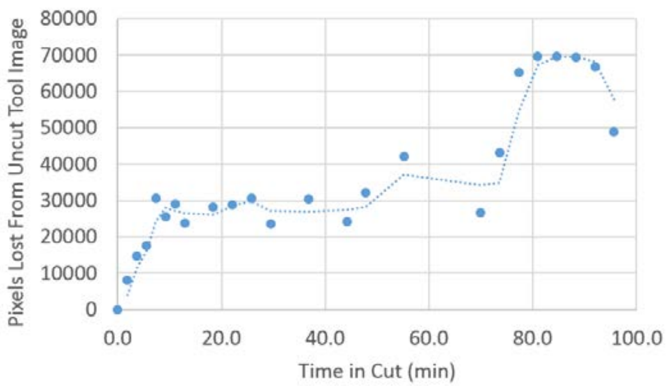

FIGURE 5. CHANGE IN TOOL'S IMAGE PIXELS FOR A SET OF TEETH ON A SINGLE FLUTE SHOWING WEAR AND TOOL EDGE LOSS DURING THE CUT. THE DATA FIT LINE IS A MOVING AVERAGE.

During these tests, it was noted that the material often produced very long chips (10-100 cell wall lengths as shown in Figure 6) demonstrating that the shredder portion of the tool was only shredding a small portion of the material into particles. The long chips shown in Figure 6 are from a relatively new tool that is still early in its cutting life, so the performance is only going to decline in the remaining 88 minutes for this tool. Additionally, during the cutting process, there was often a sound that could best be described as a high pitched rubbing sound. These observations showed the need for a better understanding of the cutting process.

FIGURE 6. CHIPS COLLECTED AT 7.4 MINUTES OF CUT TIME - SCALE AT BOTTOM OF IMAGE IS MM

In an attempt to better understand the mechanism causing the generation of long chips and rubbing sounds, the standard frame rate video was studied. Immediately, it was noted that cutting only occurred at locations where the honeycomb was made geometrically stiffer by the intersection of multiple walls. In areas between these intersections, the individual wall sections would tear loose at the depth of cut creating a flag of at least 1 cell wall length that would rub against the tool at least until the tool had progressed to the next wall intersection. This indicated that the stiffness of the material in a single wall was not sufficient to generate the shear stress required to cut the material on the cutting edge of the tool. While the standard frame rate video appeared to show some of the mechanisms occurring, to really understand what was happening during the cutting process, it was decided that high speed videography was required.

HIGH SPEED VIDEO EVALUATION OF CUTTING

Table 3 shows the specifications of the high speed camera and the video parameters for most of the videos collected. Videos were taken for many combinations of cutting parameters and from 2 primary viewpoints for each set. The first was a view normal to the side of the honeycomb block and perpendicular to the feed direction of the axis as shown in Figure 7. The second view was taken by using a mirror mounted at an approximately 45° angle above the material. This gave a view that was largely looking down on the top surface of the honeycomb along the axis of the tool as shown in Figure 8. There was a bit of an oblique offset because of the locations available for locating the camera where the mirror image was not being blocked by the tool itself. While the oblique offset makes it more challenging to accurately measure lengths from the video, it gives a perspective that is more informational to the cutting process.

The high speed video immediately showed that the previous understanding of the material cutting at each supporting intersection was incomplete. The rubbing hypothesis had been formed with an assumption that the intersections would act as fixed mounts for the single wall section flaps of material. This assumption included the single wall section undergoing an Euler type bending that caused them to be incapable of holding their position sufficiently to generate the cutting edge stress required for the tool to cut the material. It also assumed a mostly normal loading along the length of the wall section. But instead, when the tool contacts the wall section, the material tears along the bottom edge (at or near the axial depth of cut) and the rotation of the tool pushes the tip of the wall section off to one side thus creating an eccentrically loaded, curved Euler beam. When one reviews the literature for curved beam solutions, one finds that an eccentrically loaded Euler beam (Equation 1), more representative of the actual cutting conditions, can only support approximately 25% of the load of an axially loaded beam (Equation 2) [9].

TABLE 3. VIDEO PARAMETERS FOR HIGH SPEED CAMERA

Camera	Photron FASTCAM SA5
Trigger Mode	Center
Resolution	448x560 pixels
Lighting	500W flood @ 6”
Frame Rate	7,500-20,000 frame/sec
Spindle Rotation frame to frame	14.0°-5.25°
Axis Movement, frame to frame	0.0085mm - 0.0032mm

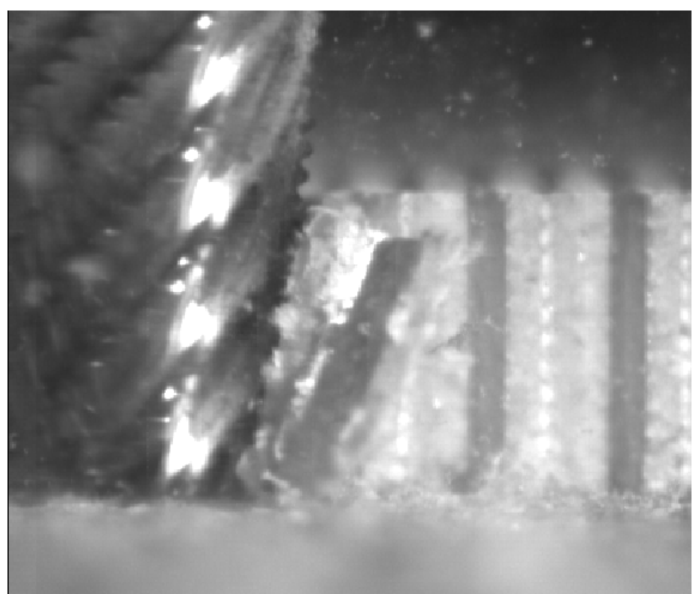

FIGURE 7. SIDE VIEW OF THE CUTTING PROCESS AS RECORDED BY THE HIGH SPEED CAMERA SHOWS A LARGE CHIP FORMING

$$P_{crit-eccentric} = 2.4674\frac{EI}{L^2} \qquad (1)$$

$$P_{crit-axial} = \frac{\pi^2 EI}{L^2} \qquad (2)$$

The high speed video also made clear, however, that the assumption of the wall intersection acting as a hinge or rigid base was also incomplete. In fact, the intersection has significant strength which is likely due to the doubling of wall thickness and the additional phenolic resin that stays in the inside corners due to surface tension. This corner resin can be seen in images in [3] though it is not mentioned in that work. Because of these effects, the bending of the wall currently being cut twists the wall intersection, thus causing the walls that are not yet under cut to also act as bent, eccentrically loaded beams that have the reduced strength and load capability from above. The twisting of a wall intersection can be seen in Figure 8 which is an image of a new tool, with total accumulated cutting time of only 1.9seconds, performing a conventional cut with the parameters previously presented. This twisting effect is considered in Gibson [7] but the end conditions for the honeycomb are constrained by the additional honeycomb in the structure from literature. In the case of machining, the honeycomb structure is being destroyed and the end conditions are not constrained in the same ways calculated otherwise. This lack of constraint allows much greater bending and deflection of the cell wall ends exhibited as a significantly reduced stiffness. This localized deformation appears to be outside of the existing literature and is also not mathematically solved in this work, but merely observed in the cutting action.

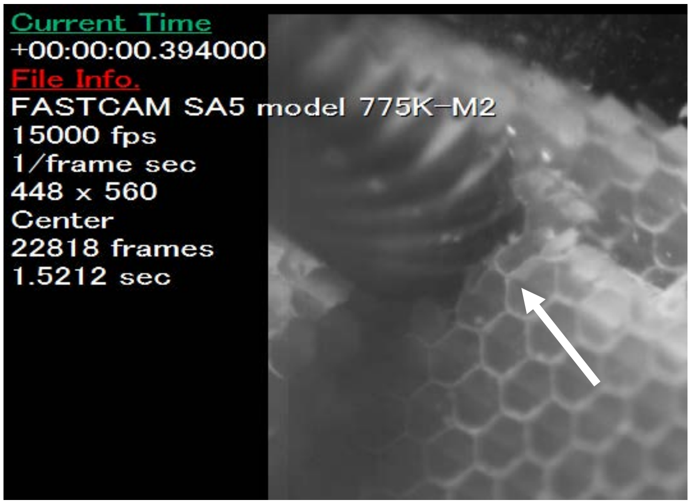

FIGURE 8. HIGH SPEED VIDEO WITH ARROW INDICATING WALL SECTIONS TWISTING UNDER THE LOADING OF TOOL ROTATION AND FEED

It is instructive to follow the cell collapse from 0.394 seconds, as shown in Figure 8, going forward for the time that it takes the tool to traverse less than a single cell's distance (2.286mm in 0.036s). The cell collapse due to bending can be seen in a series of video images. Because the collapse and motion of individual wall sections is difficult to track in separate print images (something that is clear in continuity of the video) the edges have been traced and are shown in Figure 9. From this figure, the cell collapse is seen to progress with each further deformation of the cell coming from a twisting of the walls to the point at 0.417 seconds that one of the walls completely doubles back upon itself where there was previously an intersection. At 0.428 seconds, the entire wall structures has crushed and bears little resemblance to the original honeycomb shape. At 0.430s, the wall which is at least 4 wall sections long, tears loose and begins to flap against the tool.

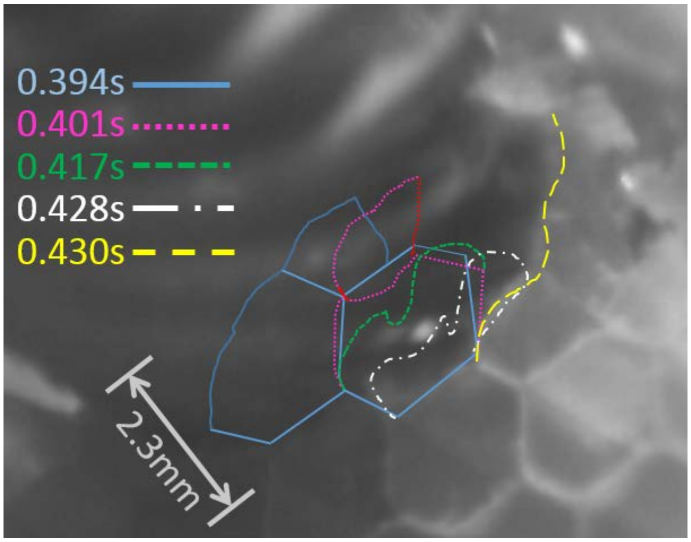

FIGURE 9. THE CELL WALL SECTIONS WERE TRACED OVER A PERIOD OF 0.036S WHILE THE TOOL MOVED 2.286MM SHOWING THE COLLAPSE OF THE CELLS

What is not evident from these images, due to the limited focal length required to achieve adequate aperture for high speed light acceptance, is that there is already a section of connected walls flapping and rubbing on the outside edge of the tool for this entire set of images. At 0.431s, this wall flap is finally cut loose as shown in Figure 10, though the wall sections in that figure are folded over. In fact, the wall is at least 5 cell wall sections long and might be longer, though it is hard to tell for certain from the video images. It is important to consider this large flap and the significant time of the flap rubbing on a brand new tool with less than 2 seconds of total cut time in its life – there is no time at which the tool should be more able to cut material effectively and to shred the chips to dust than when new and completely unworn. As the tool becomes duller and the shear pressure reduces with rounding of tool edges, the ability to cut will only decrease and this reduction in cutting ability was seen in the chips produced and collected throughout the cutting process.

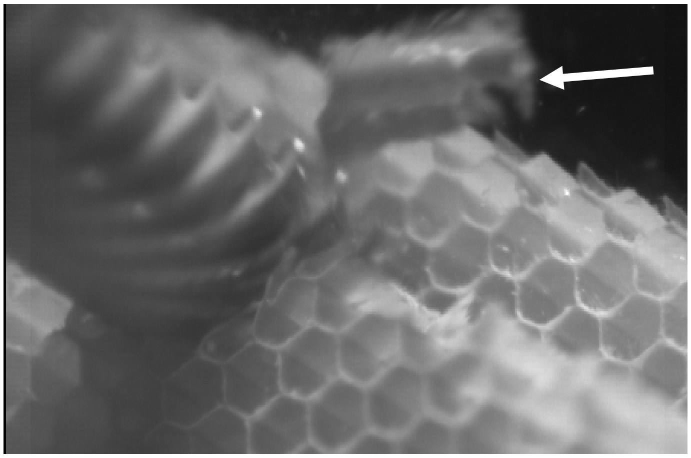

FIGURE 10. THE FLAP OF CELL WALLS (SEE ARROW) IS CUT LOOSE FROM THE HONEYCOMB AT 0.431S

In most cutting processes, the heat generated in the cutting process is the primary driver of wear. As temperature increases, the hardness and strength of the cutting material decreases and the cutting edge is worn away. Therefore, the team attempted to measure the cutting temperature. An infrared (IR) camera was used to measure temperature while cutting, but the high rotational speed of the tool and the relatively slow shutter speed of the IR appeared to cause averaging between the hot cutting edges and the relatively cool bulk of the tool. Attempts to stop the tool quickly after cutting also failed to produce results. Either the cooling of the tool was too fast or the resolution of the camera was not sufficient to separate the emission of the cutting edges of the tool from the bulk of the tool. While temperature changes were evident, the measured temperatures were not of a magnitude sufficient to cause any tool wear acceleration. Because the bulk of the tool warmed by 10's of degrees during the short cutting passes, it is indirectly inferred that the temperature at the edges is quite significant and that a different temperature measurement method is required. Most prior tool temperature measurements in literature have been achieved in single point cutting applications on lathes. The team attempted this as well but could not replicate the flapping and rubbing without a rotating tool. This discussion is included because an accurate temperature measurement is believed to be important to the understanding of wear in this process, but wasn't achieved through multiple efforts. Options to achieve this measurement in the future might include a high shutter speed camera with significantly increased resolution, or possibly a fiber optic based system capable of highly localized measurements.

Finally, the inability of the tool to remove the entire cell wall material with even a new, sharp tool would suggest that the shredder section of the tool is not working as intended. Because the shredder near the top of the cut is causing a rotation and deflection of the walls, walls are bending and the wall intersections are twisting which causes them to not be able to generate the stress necessary at the tool's cutting edge to cleanly separate from the bulk material. A different strategy may be needed to achieve the maximum tool life and to reduce the rubbing of cell wall material on the sides of the tool. An observation from the high speed video of the cutting process was of the passage of the cutting flutes as see through deflection of the honeycomb material. When the cells were collapsing, the deflections in the material clearly showed the location of the cutting flutes passing behind the collapsed walls (from the camera's perspective). The qualitative observation was that the wall seemed to be resting across many cutting flutes simultaneously because of the very high pitch angle of the flutes and the high number of cutting flutes in contact with the cell wall at any time. It is proposed, but not tested here, that if the pitch angle were decreased (more aligned with the tool axis) and the number of cutting flutes decreased, the wall structure would see increased stress at the tool edge which might be more likely to induce the shear required to cut the material and reduce the amount of rubbing observed in these tests.

CONCLUSIONS

Tool wear of cutting tools used for the sculpting of Nomex aramid honeycomb was studied through performing cutting tests. These tests showed the tool to experience a rapid change in tool geometry over the first 7.4 minutes of cutting followed by a plateau in which the tool geometry did not significantly change. When 73 minutes in cut had elapsed, the tool began to suffer rapid wear and geometry change with the loss of multiple cutting edges. The tool was finally deemed unusable at 96 minutes when it began to wrap long chips and tear out large sections of honeycomb. These tests showed the cutting life of these expensive tools to be relatively short, while also indicating that the tool was often collapsing honeycomb cells rather than cutting them. High speed video was used to evaluate the cutting process and showed the tool to be applying twisting motions to the cell wall sections that transferred through the cell wall intersections. This bending caused the cell walls to have reduced stiffness well before the cutting tool arrived, leading to a collapse of the wall structure ahead of the tool. This appears to eventually cause long flags of connected cell wall sections to spend a significant amount of time flapping and rubbing against the tool, potentially causing wear through abrasion and heat generation, though the heat generation could not be confirmed adequately. These results suggest that an alternative method of cutting might be preferable if it reduces twisting of the wall intersections long before the arrival of the tool. Suggestions include lower flute helix angle and a reduced number of cutting edges.

ACKNOWLEDGMENTS

The authors would like to acknowledge Hexcel, Inc. for providing tools and Nomex honeycomb for this work, ITRONX for providing guidance and additional days of high speed camera usage, and Controx-Neuhauser for providing tools at reduced cost.

REFERENCES

1. Palanikumar, K. and J.P. Davim, *Assessment of some factors influencing tool wear on the machining of glass fibre-reinforced plastics by coated cemented carbide tools*. Journal of Materials Processing Technology, 2009. **209**(1): p. 511-519.
2. Takeyama, H. and N. Iijima, *Machinability of Glassfiber Reinforced Plastics and Application of Ultrasonic Machining*. CIRP Annals - Manufacturing Technology, 1988. **37**(1): p. 93-96.
3. Seemann, R. and D. Krause. *Numerical modelling of nomex honeycomb cores for detailed analyses of sandwich panel joints*. in *11th World Congress on Computational Mechanics (WCCM XI)*. 2014.
4. de Lacalle, L.N.L., et al., *Design and Test of a Multitooth Tool for CFRP Milling*. Journal of Composite Materials, 2009. **43**(26): p. 3275-3290.
5. Society of Automotive Engineers, S.I., *AMS-STD-401: Sandwich Constructions and Core Materials; General Test Methods*. 1999-01-01.
6. Hexcel, I., *HexWeb HRH-10 Product Data Sheet*.
7. Gibson, L.J. and M.F. Ashby, *Cellular Solids: Structure and Properties*. 2nd ed. Cambridge Solid State Science Series. 1997, Cambridge, U.K.: Cambridge University Press. 510.
8. Tools, C.-N.P.C., *Tools for the Machining of Composite Materials*. 2014: Springfield, OH.
9. Ugural, A.C. and S.K. Fenster, *Applied Strength and Elasticity*. 3 ed. 1995, Upper Saddle River, New Jersey, USA: Prentice Hall PTR.